LOCALIZED FUNCTIONAL NEUROIMAGING RETRIEVAL USING 3D DISCRETE CURVELET TRANSFORM

Sidong Liu[1], *Weidong Cai*[1], *Lingfeng Wen*[1,2], *Stefan Eberl*[1,2], *Michael J Fulham*[1,2,3], *Dagan Feng*[1,4]

[1] Biomedical and Multimedia Information Technology (BMIT) Research Group, School of Information Technologies, University of Sydney, Australia
[2] Department of PET and Nuclear Medicine, Royal Prince Alfred Hospital, Sydney, Australia
[3] Sydney Medical School, University of Sydney, Australia
[4] Centre for Multimedia Signal Processing (CMSP), Department of Electronic & Information Engineering, Hong Kong Polytechnic University, Hong Kong

ABSTRACT

Neuroimaging is a fundamental component of the neurological diagnosis. The greatly increased volume and complexity of neuroimaging datasets has created a need for efficient image management and retrieval. In this paper, we advance a content-based retrieval framework for 3D functional neuroimaging data based on 3D curvelet transforms. The localized volumetric texture feature was extracted by a 3D digital curvelet transform from parametric image of cerebral metabolic rate of glucose consumption with a set of adaptive disorder-oriented masks for each type of neurological disorder. The results, using 142 clinical dementia studies, show that our proposed approach supports efficient and high performance neuroimaging data retrieval.

***Index Terms*—**3D digital curvelet transform, localized retrieval, functional imaging, brain imaging

1. INTRODUCTION

Functional neuroimaging, such as position emission tomography (PET), offers important insights into neurobiology and is used in clinical neurological diagnosis and patient care. Advances in scanning instrumentation in recent years have led to large neuroimaging datasets with greatly increased volume and complexity. Therefore, there is a need for efficient neuroimaging data management and retrieval approaches.

Retrieval of neurological images based on visual/ physiological content could provide an alternative to the traditional text search approach which is based on clinicians' annotations and patients' demographic information [1, 2]. A variety of content-based image retrieval (CBIR) systems for neurological images have been reported. Wong *et al*. [3] built a neuro-informatics database system (NIDS) with co-registered static PET and MR image data for temporal lobe epilepsy studies. Their system supported retrieval by geometric location, metabolic counts of glucose consumption and keywords from the file header. Batty *et al.* [4] developed a prototype semantic retrieval system for brain PET images using Gabor filters based texture features and a mean index ratio extracted from the predefined regions of interest (ROIs).

In the CBIR domain, the curvelet transform has been reported as a superior image representation technique over many other traditional image representation techniques, such as wavelet, ridgelet and Gabor filters [5-7]. We recently proposed a neuroimaging CBIR system that implemented the digital curvelet transform (DCvT). Our approach took physiological data into consideration by using the cerebral metabolic rate of glucose consumption (CMRGlc). We also constructed a set of disorder-oriented masks (DOMs) to further enhance the retrieval. The results of our study showed that DCvT was an effective and efficient tool in brain image retrieval and our system could achieve high accuracy by using as few as 12 curvelet coefficients to represent one image [8].

However, our previous system was only applied to 2D images without taking advantage of rich 3D information in the images. To further capture the volumetric properties in the 3D neuroimaging data, in this study, we advance our CBIR framework using 3D discrete curvelet transform (3D-DCvT). Our preliminary results suggest that the 3D-DCvT based approach could capture the volumetric information which was missed by the 2D feature extraction methods, thereby enhancing 3D neuroimaging data retrieval.

2. METHODS

2.1. 3D Neuroimaging Data Pre-processing

The CMRGlc parameters from raw static 3D FDG ([^{18}F]*2-fluoro-deoxy-glucose*) PET images were derived with the autoradiographic (ARG) algorithm [9]. Arterialized-venous blood samples were taken at 10 min and 45 min post injection to calibrate a population-based input function [10]. To eliminate the inconsistencies between different cases and

facilitate functional mapping, the generated CMRGlc parametric image volume with dimensions of 128×128×56 were spatially normalized to a PET brain template with standard dimensions of 91×109×91, using the SPM2 package (Wellcome Trust Centre for Neuorimaging, London, U.K.) [11]. The MNI-based Tzourio-Mazoyer atlas [12] was then used to define 116 functional volumes of interest (VOI), including 45 VOIs for each hemispheres, 18 VOIs for cerebellum and 8 VOIs for the cerebellar vermis.

2.2. Construction of Disorder-Oriented Masks (DOMs)

To extract the VOIs functionally related to the disorders, we defined a set of initial DOMs. Each DOM was a subset of the Tzourio-Mazoyer atlas and contained the VOIs related to certain disorders which were classified by expert clinical opinion. The initial DOMs were further refined by the t-map [13], which was a parametric image derived by translating all voxel values into values in a normal distribution. The mean and standard deviation of the age-matched control subjects were used to calibrate the distribution function. For a given threshold (p-value << 0.05), the abnormal voxel values compared with age-matched controls were retained and values in a normal range were set to zero. If the non-zero voxel values of a t-map were not included in the initial DOMs, the locations of these voxels were added to the corresponding DOMs.

2.3. 3D Discrete Curvelet Transform (3D-DCvT)

Curvelet transform is a multiscale image representation approach developed by Candes and Donoho [5]. Based on the continuous curvelet transform, Candes *et al.* further proposed the digital Curvelet transform (DCvT) for providing a simpler, faster and more accurate construction operation on digital data [14]. The 3D-DCvT proposed by Ying *et al.* [15] was an extension to the 2D-DCvT.

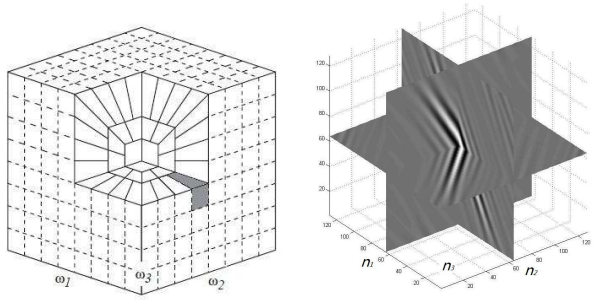

Fig.1 (a) Curvelet in frequency domain; (b) Curvelet in spatial domain.

Like the 2D curvelet, a 3D curvelet can be defined by a scale parameter *j*, an orientation parameter *l*, and a translation parameter *k* in frequency domain as follows:

$$\tilde{\varphi}^{D}_{j,l,k}(\omega) = U_{j,l}(\omega) e^{i\left\langle x_k^{(j,l)},\omega\right\rangle} \quad \textbf{(1)}$$

where $\omega = (\omega_1, \omega_2, \omega_3)$ are the frequencies variables and $e^{i\left\langle x_k^{(j,l)},\omega\right\rangle}$ represents the translation of the curvelet at position *k*, $k = (k_1, k_2, k_3)$. $U_{j,l}$ is a discrete frequency window which isolates frequencies near scale *j* and direction *l*, as shown in Fig.1 (a). Fig.1 (b) shows the corresponding curvelet in spatial domain. The frequency window is expressed by:

$$\begin{cases} \tilde{U}_{j,0}(\omega) = \tilde{W}_j(\omega), & \text{at the coarsest and the finest scales,} \\ \tilde{U}_{j,l}(\omega) = \tilde{W}_j(\omega) \cdot \tilde{V}_{j,l}(\omega), & \text{at other scales,} \end{cases} \quad \textbf{(2)}$$

where $\tilde{W}_j(\omega)$ and $\tilde{V}_{j,l}(\omega)$ correspond respectively to the radial and angular frequency windows.

For a given 3D volumetric image $f(n_1, n_2, n_3)$, $0 \le n_1, n_2, n_3 \le n$, we first applied the 3D fast Fourier transform (FFT) and obtained Fourier samples, $\tilde{f}(\omega_1, \omega_2, \omega_3)$, $-n/2 \le \omega_1, \omega_2, \omega_3 \le n/2$. For each scale *j* and angle *l*, we formed the product $\tilde{U}_{j,l}(\omega) \cdot \tilde{f}(\omega)$. Then we wrapped this product around the origin to obtain $W(\tilde{U}_{j,l} \cdot \tilde{f})(\omega)$ except for the finest and the coarsest scales. Finally, we applied a 3D inverse FFT to each $W(\tilde{U}_{j,l} \cdot \tilde{f})$, hence collecting the discrete coefficients $c^D(j,l,k)$ defined in frequency domain by

$$c^D(j,l,k) := \frac{1}{(2\pi)^2} \int \tilde{f}(\omega) \overline{\tilde{\varphi}^D_{j,l,k}(\omega)} d\omega \quad \textbf{(3)}$$

3D-DCvT can be implemented by in-core, out-of-core, or the MPI-based parallel approaches [15]. The selection of different implementations depends on the image dimensions. Since the in-core approach is more suitable for an image with small dimensions, we used the in-core approach to perform the curvelet transforms.

2.4. Localized 3D-DCvT Based Multiscale Texture Feature Extraction

The 3D-DOMs derived in Section 2.3 were applied to all the 3D parametric images to extract the pathological VOIs. The regions not covered by the DOMs were filtered out before calculating the feature vectors. The mean and standard deviation of the selected Curvelet transform coefficients were computed to construct the feature vectors. If *m* curvelets were used, then a feature vector would contain *2m* elements. The dimensions of DOM-based image data were 91×109×65, so we could decompose the image up to 6 sub-bands/scales ($65 \approx 2^6$). However, the redundant data created with a large number of scales could reduce the distinguishing power of the feature vectors [16] and poses a great computation burden. Therefore, we ignored the sixth scale and defined 29 curvelets across 5 scales as follows: at the coarsest scale and the least coarse scale, a single curvelet

was defined by default; for other scales, we selected 3 out of 6 curvelets at the second coarsest scale, 12 out of 24 curvelets at the third coarsest scale, and 12 out of 24 curvelets at fourth coarsest scale. Such half-size settings related to the symmetry property of curvelet transform. Therefore, a 58-element feature vector was extracted to represent each 3D neurological image.

The extracted 58 elements in the feature vectors had very different ranges for their values. To eliminate the range disparity between different feature spaces, we first chopped off the top 5% of the distribution within each feature space because these extreme values most likely resulted from noise. Then we divided all the values within the feature space by the nominal maximum of the rest of the 95% elements to make distance measured among different feature spaces on the same basis.

3. EVALUATION

Table 1 Dataset of patients with suspected dementia

Disorder Type	Cases (Male : Female)	Age Range
AD	38 (17:21)	51-73
FTD	37 (21:16)	53-74
AD/DLBD	12 (5:7)	55-73
Other Disorders	39 (19:18)	50-75
Normal	18 (11:7)	53-75
Total	**142 (73:69)**	**50-75**

The patient datasets, shown in Table 1, were acquired on a CTI ECAT 951R whole body PET scanner, at the Department of PET and Nuclear Medicine, Royal Prince Alfred Hospital. The two main subtypes of dementia, frontal-temporal dementia (FTD) and Alzheimer's disease (AD), were investigated. The "AD/DLBD" cases were claimed as 'indefinite', because there were patterns of glucose hypometabolism consistent with AD and Diffuse Lewy Body Disease (DLBD).

We used the diagnosis from the imaging study as the ground truth. For some subtypes of dementia, there can be a degree of overlap because similar brain regions are affected. To balance the impact caused by common regions shared by different disorders and to objectively describe the retrieval results, the following relevance criteria shown in Table 2 were considered.

Table 2 The relevance criteria

SCORE	CRITERIA
1.0	The retrieval image belongs to the same class as the query image
0.75	The retrieval image belongs to AD/DLBD disorder, if the query image is an AD case
0.25	The retrieval result belongs to any other disorder class except the classes it belongs or relates to
0.0	The retrieved image belongs to normal class

The similarity was calculated by the Euclidean distance and leave-one-out paradigm was adopted in this study on the whole dataset. The retrieval performance was evaluated by the precision versus number of retrieval results curves. To verify the effectiveness of 3D-DCvT, we compared our proposed approach to the 2D-DCvT based approaches using the global features (i.e., whole-brain based features without DOMs).

4. RESULTS

Fig. 2 shows the retrieval results of using 2D-DCvT based approaches and 3D-DCvT based approaches for AD cases (*-DCvT_AD) and FTD cases (*-DCvT_FTD). All the approaches shown in Fig.2 were based on global features. In other words, the comparison between 2D- and 3D- DCvTs was conducted without the impact of the DOMs. For both AD and FTD cases, the proposed 3D-DCvT based approaches (solid lines) greatly outperformed the 2D-DCvT based approaches (dotted lines).

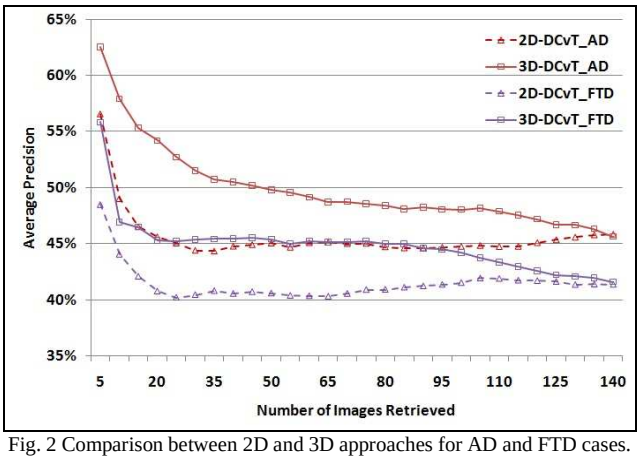

Fig. 2 Comparison between 2D and 3D approaches for AD and FTD cases.

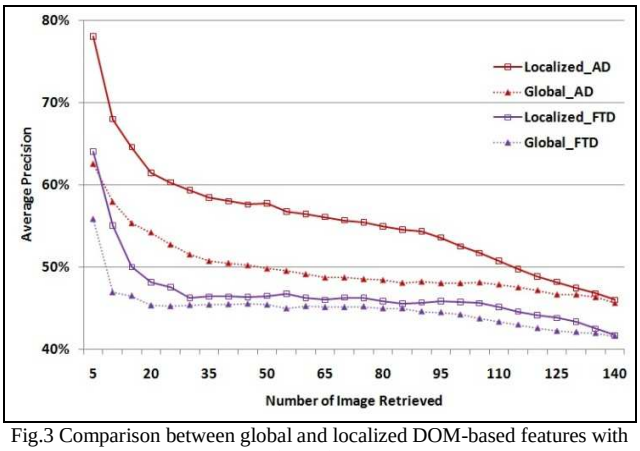

Fig.3 Comparison between global and localized DOM-based features with 3D-DCvT.

Fig. 3 shows the comparison of localized DOM-based features and global features extracted by 3D-DCvT

approaches. For both the AD and FTD cases, the performance of using localized DOM-based features (solid lines) was higher than that of using global features (dotted lines), and the improvement for the retrieval of AD cases was striking.

In regard to the computation complexity, we found that for a laptop computer with 3GB of memory and a 3.0 GHz CPU, it took 5.1 seconds on average to process one full-sized image volume with dimensions of 91×109×91 and 3.5 seconds to process a DOM-based image with dimensions of 91×109×65.

5. CONCLUSION

In this paper, we extended our CBIR approach using DCvT for 3D neuroimaging data. To our knowledge, it is the first time that 3D-DCvT had been used in the CBIR domain. A set of DOMs were also constructed to select the VOIs for each subtype of dementia. The findings from our experimentation indicated that the 3D-DCvT based approaches could capture the innate volumetric property which was beyond the scope of 2D methods, hence achieving more accurate retrieval. In addition, the localized features extracted from DOMs could filter out the non-VOI regions, and further enhance the neuroimaging retrieval.

6. ACKNOWLEDGEMENT

This work was supported in part by ARC and PolyU grants.

7. REFERENCES

[1] H. Muller, N. Michoux, D. Bandon, and A. Geissbuhler , "A review of content-based image retrieval systems in medical applications – clinical benefits and future directions," *International Journal of Medical Informatics*, vol. 73, pp.1-23, 2004.

[2] L.R. Long, S. Antani, T.M. Deserno, and G.R. Thoma, "Content-based Image Retrieval in Medicine: Retrospective Assessment, State of the Art, and Future Directions", *International Journal of Healthcare Information Systems and Informatics*, vol. 4, no. 1, pp.1-16, 2009.

[3] S.T.C. Wong, K.S. Hoo, X. Cao, D. Tjandra, J.C. Fu, and W.P. Dillon, "A neuroinformatics database system for disease-oriented neuroimaging research", *Academic Radiology*, vol. 11, no. 3, pp.345-358, 2004.

[4] S. Batty, J. Clark, T. Fryer, and X. Gao, "Prototype system for semantic retrieval of neurological PET images", *The International Conference on Medical Imaging and Informatics (MIMI 2007), Aug 14-16, 2007, Beijing*, LNCS 4987, pp.179-188, 2008.

[5] E.J. Candes, D.L. Donoho, "Curvelets – a surprisingly effective nonadaptive representation for objects with edges", *Curves and Surfaces*, pp.105-120, Vanderbilt University Press, Nashville, TN, 2000.

[6] L. Dettori, L. Semler, "A comparison of wavelet, ridgelet and curvelet based texture classification algorithms in computed tomography", *Computers in Biology and Medicine*, vol.37, pp.486-498, 2007.

[7] I.J. Sumana, M.M. Islam, D. Zhang, and G. Lu, "Content based image retrieval using Curvelet transform," *The Proc. of Int. Workshop on MMSP*, Oct, 2008.

[8] S. Liu, L. Jing, W. Cai, L. Wen, S. Eberl, M.J. Fulham, and D. Feng, "Localized Multiscale Texture Based Retrieval of Neurological Image", *Proc. 23rd IEEE International Symposium on Computer-Based Medical Systems (CBMS 2010)*, Australia, pp.243-248, 2010.

[9] G.D. Hutchins, J.E. Holden, R.A. Koeppe, J.R. Halama, S.J. Gatley, and R.J. Nickles, "Alternative approach to single-scan estimation of cerebral glucose metabolic rate using glucose analogs with particular application to ischemia", *Journal of Cerebral Blood Flow and Metabolism*, vol. 4, pp.35-40, 1984.

[10] S. Eberl, A.R. Anayat, R. Fulton, P.K. Hooper, and M.J. Fulham, "Evaluation of two population-based input functions for quantitative neurological FDG PET studies", *European Journal of Nuclear Medicine*, vol. 24, no. 3, pp.299-304, 1997.

[11] R.S.J. Frackowiak, K.J. Friston, C.D. Frith, R.J. Dolan, C.J. Price, S. Zeki, J.T. Ashburner, and W.D. Penny, *Human Brain Function*. Amsterdam; Boston: Elsevier Academic Press, 2004.

[12] N. Tzourio-Mazoyer, B. Landeau, and D. Papathanassiou, "Automated Anatomical Labeling of Activations in SPM Using a Macroscopic Anatomical Parcellation of the MNI MRI Single-Subject Brain", *NeuroImage*, vol. 15, no. 1, pp. 273-289, 2002.

[13] W. Cai, S. Liu, L. Wen, S. Eberl, M.J. Fulham, and D. Feng, "3D neurological image retrieval with localized pathology-centric CMRGlc patterns", *The Int. Conf. on Image Processing (ICIP 2010)*.

[14] E.J. Candes, L. Demanet, D. Donoho, and L. Ying, "Fast Discrete Curvelet Transforms", *Multiscale Modeling and Simulation*, vol. 5, no.3, pp. 861-899, 2006.

[15] L.Ying, L. Demanet, and E. Candes, "3D Discrete Curvelet Transform," in *Proceedings of the International Society for Optical Engineering (SPIE)*, 2005.

[16] M.M Eltoukhy, I. Faye, and B.B Samir, "Breast cancer diagnosis in digital mammogram using multiscale curvelet transform", *Computerized Medical Imaging and Graphics*, vol. 34, no.4, pp. 269-276, June 2010.